

Original Article

## The synthesis of imprinted polymer sorbent for the removal of mercury ions

Djabal Nur Basir<sup>1,2</sup>, Muhammad Ali Zulfikar<sup>1</sup>, and Muhammad Bachri Amran<sup>1\*</sup>

<sup>1</sup> Analytical Chemistry Research Group, Institut Teknologi Bandung, Bandung, 40132 Indonesia

<sup>2</sup> Department of Chemistry, Universitas Hasanuddin, Makassar, 90124 Indonesia

Received: 18 March 2019; Revised: 6 June 2019; Accepted: 29 July 2019

---

### Abstract

In order to remove mercury ions, Hg(II)-ion-imprinted polymers (Hg-IIPs) with silica core were synthesized by radical polymerization using complexes of Hg(II) ions with 3-mercaptopropyltrimethoxysilane ligands as a template, vinyl-trimethoxysilane as a monomer, and ethylene glycol dimethacrylate as a crosslinker, in the molar ratio 1: 6: 6. Silica, thiol, vinyl, carbonyl, and Hg(II) in the synthesis process were detected through FTIR, SEM-EDS, TGA, and BET analyses. Using Hg-IIPs as the sorbent, mercury ion removal was near optimal from a batch at pH 4 with an interaction time of 90 min, and gave 62.27 mg.g<sup>-1</sup> adsorption capacity. The capture by Hg-IIPs of Hg(II) ions in the presence of Pb(II), Cd(II), and Cu(II) ions in quaternary solutions had the selectivity coefficients 46.92 for Hg/Cu, 16.82 for Hg/Cd, and 2.07 for Hg/Pb.

**Keywords:** removal, mercury, Hg-IIPs

---

### 1. Introduction

Mercury is among the most toxic heavy metals that can endanger human health, and it can enter the body orally, through skin, or by inhalation (Risher & Amler, 2005). The bioaccumulation or progressive increase of mercury in natural aquatic ecosystems, with further enrichment on passing through the food chain, can have detrimental effects on humans exposed through consumption of contaminated food, such as fish and shellfish. Currently common methods of mercury removal include liquid-liquid extraction (Didi, Medjahed, & Benaoudam, 2013), solid phase extraction (Escudero, Olsina, & Wuilloud, 2013), membrane filtration (Urgun-Demirtas *et al.*, 2012), and flotation separation (Ghazy, El-Reash, Al-Gammal, & Yousef, 2010).

Solid phase extraction (SPE) is a multipurpose method that has been widely used in adsorption, separation and preconcentration processes. When compared to solvent extraction SPE has several advantages, being a relatively

faster and easier-to-use process, demanding less organic solvents, providing better preconcentration and selectivity, and it can be used with analytical instruments such as AAS, CVAAS, HPLC, and ICP-OES (Soleimani, Mahmodi, Morali, Khani, & Afshar, 2011). Molecularly imprinted polymers (MIPs) as novel SPE sorbents have appeared as an alternative for the purpose of achieving more selective adsorption of analyte targets (Wulandari, Urraca, Descalzo, Amran, & Moreno-Bondi, 2015). The MIPs have become an established technique for preparing strong molecular recognition elements for a variety of target molecules. Currently, the use of ion-imprinted polymers (IIPs) as functional materials that are selective sorbents in adsorption, separation, and preconcentration of metal ions, is the latest driver in SPE innovations. Molecular imprinting is the process of forming a print on a material (binder or catalyst) so that it has a specific recognition site, where the print is used to direct both position and orientation of the target molecule in a self-assembly mechanism (Piletsky, Turner, & Laitenberger, 2006). Compared with other sorbents in SPE, IIPs have the advantages of using only a small number of polymers that can be reused, minimizing the loss factor of the analyte, easy preparation, having relatively high resistance to temperature and che-

---

\*Corresponding author

Email address: amran@chem.itb.ac.id

micals, and having a high level of selectivity. The high selectivity of IIP is caused by memory effects of size, geometry, coordination number, and charge of the metal ion (Singh & Mishra, 2009) that the interaction of metal ions with specific ligands provide to a polymer. Prior studies have used a radical polymerization strategy with different monomers and ligands to form ion-imprinted polymers for Hg(II) ions (Firouzzare & Wang, 2012; Hasemi *et al.*, 2015; Roushani, Abbasi, & Khani, 2015).

In this work, the strategy is to trap Hg(II) ions in a polymer matrix using 3-mercaptopropyltrimethoxysilane (MPTS) ligands. The SH groups in the ligand will interact by covalent bonds with Hg(II) ions, and the other side of the ligand will bind to the silica core through hydrolysis, while for polymerization vinyltrimethoxysilane (VTMS) is used as the monomer and ethylene glycol dimethacrylate (EGDMA) as the crosslinker. After the Hg(II) ions have been released from the polymer matrix to obtain Hg(II)-ion imprinted polymers (Hg-IIPs), the imprints left behind are selective for Hg(II) ions. So, the Hg-IIPs can be used as selective sorbents for adsorption, separation, and preconcentration of mercury ions.

## 2. Materials and Methods

### 2.1 Materials

The materials used in this work include: Hg(NO<sub>3</sub>)<sub>2</sub>.H<sub>2</sub>O (Merck), Silica gel (SG, Merck), tetraethoxysilane (TEOS, Aldrich), 3-mercaptopropyltrimethoxysilane (MPTS, Aldrich), vinyltrimethoxysilane (VTMS, Aldrich), ethylene glycol dimethacrylate (EGDMA, Aldrich), benzoyl peroxide (BPO, Merck), ethanol (Merck), acetonitrile (Merck), HNO<sub>3</sub> (Merck), HCl (Merck), Thiourea (Merck), NH<sub>3</sub> 25% (Merck), SnCl<sub>2</sub>.2H<sub>2</sub>O (Merck), Pb(NO<sub>3</sub>)<sub>2</sub> (Merck), Cd(NO<sub>3</sub>)<sub>2</sub>.4H<sub>2</sub>O (Aldrich), Cu(NO<sub>3</sub>)<sub>2</sub>.3H<sub>2</sub>O (Merck), and distilled water.

### 2.2 Pre-polymerization: The synthesis of SG-TEOS, HMPTS, ST-HMPTS, and ST-HMPTS-VTMS

2 g of SG was added with 10 mL of 25% NH<sub>3</sub>, 40 mL of distilled water, 25 mL of ethanol, and 5 mL of TEOS, stirred at 200 rpm for 6 h, and then placed in an oven at 70°C for 6 h to obtain the silica core (SG-TEOS).

Hg(NO<sub>3</sub>)<sub>2</sub>.H<sub>2</sub>O and MPTS in molar ratio 1: 4 were dissolved in 10 mL of acetonitrile and stirred at 200 rpm for 30 min to obtain a polymer template (HMPTS).

For further work, the composition of HMPTS (template), VTMS (monomer), and EGDMA (crosslinker) was in the molar ratio 1: 6: 6. Table S-1 summarizes the effects of adding a crosslinking agent on adsorption capacity by composition.

The synthesis from 20 mg of SG-TEOS and HMPTS by hydrolysis was carried out with 40 mL of distilled water, 25 mL of ethanol, and 10 mL of 25% NH<sub>3</sub> while stirring at 200 rpm for 7 h, and then ST-HMPTS was obtained.

The hydrolysis was carried out in the same manner between ST-HMPTS and VTMS in 40 mL of distilled water, 25 mL of ethanol, and 10 mL of 25% NH<sub>3</sub> under stirring at 200 rpm for 7 h, and then ST-HMPTS-VTMS was obtained.

### 2.3 Polymerization: The synthesis of IIPs, Hg-IIPs, and NIPs

The synthesis of ion-imprinted polymers (IIPs) utilized ST-HMPTS-VTMS and EGDMA in 30 mL of acetonitrile purged with N<sub>2</sub> gas for 3 min, and then 125 mg of BPO was added and heated at 70°C with stirring at 200 rpm for 1 h. The leaching of Hg(II) ions in IIPs gave Hg(II)-ion imprinted polymers (Hg-IIPs), and was done with a mixture of 100 mL of 4 M HNO<sub>3</sub> and 2% of thiourea for 24 h, in 2 cycles. Furthermore, the same leaching process was carried out for 24 h in 2 cycles using 100 mL of 2 M HNO<sub>3</sub>. The Hg-IIPs formed by leaching were then washed with ethanol and distilled water, and then dried at room temperature and in an oven at 60°C for 6 h, after which the product was sieved through mesh 60 sifted to obtain a sorbent for removing mercury ions.

The synthesis of non-imprinted polymers (NIPs) follows the stages of pre-polymerization and polymerization with similar molar proportions as in Hg-IIPs, but without the presence of Hg(II) ions.

### 2.4 Physical characterization

The synthesized products were examined by FTIR Prestige-21 (Shimadzu, Japan) over the wave number range 4000-400 cm<sup>-1</sup>. The surface morphology and the presence of chemical elements in IIPs, Hg-IIPs, and NIPs were investigated using scanning electron microscopy-energy dispersive spectroscopy (SEM-EDS) SU3500 (Hitachi, Japan). The surface area, the total pore volume, and the average pore radius of the IIPs, Hg-IIPs, and NIPs were measured using a Brunauer-Emmett-Teller (BET) analyzer (Quantachrome NOVA 3200e, Austria). The thermal stabilities of IIPs and Hg-IIPs were assessed using a thermogravimetric analyzer (NETZSCH STA 449 F1 Jupiter, German).

### 2.5 Characterization of removing mercury ions from aqueous solutions

#### 2.5.1 Effect of pH

50 mg Hg-IIPs was placed in a 50 mL Erlenmeyer flask and then left to interact with 25 mL of Hg(II) 40 mg.L<sup>-1</sup> for 2 hours on a 150 rpm shaker with pH in range from 1 to 7. The filtrate was separated from the sorbent, and measured for mercury content by cold vapor atomic absorption spectrometry (CVAAS). The same procedure was also carried out with the NIPs.

#### 2.5.2 Effect of interaction time

50 mg Hg-IIPs was placed in a 50 mL Erlenmeyer flask and then left to interact with 25 mL of Hg(II) 40 mg.L<sup>-1</sup> at pH 4 on a 150 rpm shaker for a controlled time of 5 to 120 min. The filtrate was then measured by CVAAS. The same procedure was also carried out with the NIPs.

#### 2.5.3 Determination of optimum adsorption capacity

25 mL Hg(II) with concentrations from 5 to 500 mg.L<sup>-1</sup> at pH 4 were placed in a 50 mL Erlenmeyer flask and

left to interact with 50 mg of Hg-IIPs on a 150 rpm shaker for 90 min. The filtrate was then measured by CVAAS. The same procedure was also carried out with the NIPs.

The removal percentage and adsorption capacity were calculated as follows:

$$\% \text{ removal} = \frac{C_i - C_e}{C_i} \times 100\% \quad (1)$$

$$q_e = \frac{C_i - C_e}{m} \times V \quad (2)$$

where  $q_e$  is the adsorption capacity ( $\text{mg}\cdot\text{g}^{-1}$ ),  $V$  is the volume of solution (L),  $C_i$  is the initial concentration of Hg(II) ( $\text{mg}\cdot\text{L}^{-1}$ ),  $C_e$  is the final concentration of Hg(II) ( $\text{mg}\cdot\text{L}^{-1}$ ), and  $m$  is the sorbent mass (g).

### 2.5.4 Effect of sorbent dose

The Hg-IIPs samples were placed in a 50 mL Erlenmeyer flasks with sample masses 25, 50, 75, and 100 mg, and each sorbent was allowed to interact with 25 mL of Hg(II)  $40 \text{ mg}\cdot\text{L}^{-1}$  at pH 4 on a 150 rpm shaker for 90 min. The filtrate was then measured by CVAAS. The same procedure was also carried out with the NIPs.

### 2.5.5 Selectivity

The selectivity of Hg-IIPs on Hg(II) ions was assessed with solutions containing several metal ions, namely Cd(II), Cu(II), and Pb(II). The selectivity of Hg-IIPs was tested by 3 different methods. In the first method, 25 mg of Hg-IIP in a 50 mL Erlenmeyer flask was allowed to interact for 90 min with 25 mL of solutions of Hg(II), Cd(II), Cu(II), and Pb(II) singly, with an ion concentration of  $1,994 \cdot 10^{-4} \text{ M}$  at pH 4. In the second method, a 25 mL of binary solution of Hg(II)/Cd(II), Hg(II)/Cu(II), or Hg(II)/Pb(II) with ion concentration of  $1,994 \cdot 10^{-4} \text{ M}$  at pH 4 was allowed to interact with 25 mg of Hg-IIPs for 90 min. In the third method, 25 mL of a solution containing all ions (quaternary solution) with each ion at  $1,994 \cdot 10^{-4} \text{ M}$  concentration and at pH 4, was allowed to interact with 25 mg of Hg-IIPs for 90 min.

Based on the obtained data, the selectivity coefficients of Hg-IIPs can be calculated:

$$D = \frac{C_i - C_e}{C_e} \times \frac{V}{m} \quad (3)$$

$$\alpha = \frac{D_{\text{Hg}}}{D_{\text{Me}}} \quad (4)$$

where  $C_i$  and  $C_e$  are the concentrations of Hg(II) ( $\text{mg}\cdot\text{L}^{-1}$  or M) in the solution before and after removal,  $V$  is volume of the solution (L),  $m$  is mass of Hg-IIPs (g),  $D_{\text{Hg}}$  and  $D_{\text{Me}}$  are distribution comparisons showing the ratio of Hg(II) to metal ions, and  $\alpha$  is the selectivity coefficient of Hg-IIPs.

## 3. Results and Discussion

### 3.1 Physical characterization of sorbents

#### 3.1.1 Fourier transform infrared spectroscopy (FTIR)

The FTIR spectra of the MPTS ligands (red curve) in the pre-polymerization stage in Figure 1 show the presence of Si-O-C groups at wave number  $1085.92 \text{ cm}^{-1}$ , and of SH (thiol) with sharp peak at  $2563.4 \text{ cm}^{-1}$ . The sharp peak then shifted to  $2571.11 \text{ cm}^{-1}$  after forming complexes with Hg(II) ions in HMPTS (blue curve).

The use of silica gel (SG) as a polymer core produces a polymer with high mechanical strength and chemical resistance, and its rigidity allows it to maintain the imprint formed (Bershtein *et al.*, 2009). The presence of a silica core was observed in the FTIR spectrum of ST-HMPTS (black curve), where vibrations of Si-O-Si, Si-OH, and OH are seen at wave numbers  $1031.92$ ,  $910.4$ , and  $3414 \text{ cm}^{-1}$ , respectively, which confirms the silica compounds.

The characteristics of FTIR spectrum changes in HMPTS, ST-HMPTS, and ST-HMPTS-VTMS with hydrolysis in the pre-polymerisation in Figure 1, shows peaks in the fingerprint area at wavenumber  $586.36 \text{ cm}^{-1}$  for ST-HMPTS, while for ST-HMPTS-VTMS (purple curve) the absorption peaks appears at wavenumbers  $3064.89$ ,  $1604.77$ , and  $1411.89$ .

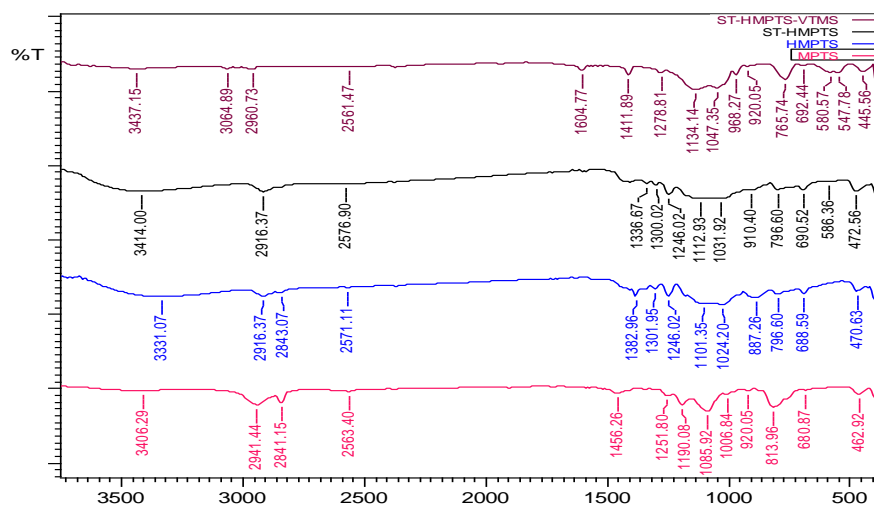


Figure 1. The FTIR spectra: MPTS (red curve), HMPTS (blue curve), ST-HMPTS (black curve), and ST-HMPTS-VTMS (purple curve).

$\text{cm}^{-1}$ , which are typical of vinyl groups.

The FTIR spectra of NIPs (black curve), IIPs (blue curve), and Hg-IIPs (red curve) are shown in Figure 2. The Hg(II) bound to the SH group in IIPs is demonstrated at wavenumber  $2576.9 \text{ cm}^{-1}$ , but leaching of Hg from IIPs to obtain Hg-IIPs caused the wavenumber to shift from  $2576.9$  to  $2555.68 \text{ cm}^{-1}$ , and a new peak at  $653.87 \text{ cm}^{-1}$  appeared for C-S bond in the fingerprint area. Similarly, in the NIPs the wavenumber of SH group was  $2533.75 \text{ cm}^{-1}$ , and the peak for C-S bond was at  $651.94 \text{ cm}^{-1}$ , both of which were similar to Hg-IIPs. Based on this, it can be concluded that the presence or absence of Hg(II) bound to the SH group only makes the peaks shift, but the C-S bond in the fingerprint area shows a significant difference, so there are two peaks for Hg-IIPs and NIPs (an area of  $650$  to  $700.16 \text{ cm}^{-1}$ ), while IIPs only give one peak ( $700.16 \text{ cm}^{-1}$ ), demonstrating that Hg(II) causes one peak for the C-S bond to disappear (Coates, 2006).

### 3.1.2 Scanning electron microscopy-energy dispersive spectroscopy (SEM-EDS)

The measurement results from SEM for NIPs, IIPs, and Hg-IIPs are shown in Figure 3. The IIPs show solid surfaces because they are filled with Hg(II), which is different from the images of Hg-IIPs that are relatively less dense (more porous) due to Hg(II) release from IIPs, showing similarity to the NIPs that also does not contain Hg(II). Table 1 shows the presence of elements C, O, Si, S, and Hg, as observed by EDS in IIPs, Hg-IIPs, and NIPs. The element C was

very dominant over the other elements, and the Hg element was successfully bound in IIPs. The absence of Hg from Hg-IIPs indicates successful leaching of Hg(II) from the IIPs, similar to NIPs that also does not contain Hg.

### 3.1.3 Thermogravimetric analysis (TGA)

Characterization by TGA was used to assess thermal stability. Regarding the loss of mass from IIPs and Hg-IIPs during temperature treatment, there could be a difference caused by leaching off Hg(II). The thermogram results in Figure 4 show three significant stages of mass loss from IIPs and Hg-IIPs, first between  $110$  and  $250^\circ\text{C}$ , then between  $250$  and  $700^\circ\text{C}$ , and finally above  $700^\circ\text{C}$ . Around  $110^\circ\text{C}$  the loss of mass was due to the release of water and volatile compounds present in both materials, and the mass of IIPs was reduced by  $5.68\%$  and the mass of Hg-IIPs by  $6.72\%$ . For up to about  $250^\circ\text{C}$  the two materials remain stable with  $94.14\%$  of IIPs mass retained, so it is relatively more stable than Hg-IIPs that retained  $92.28\%$ . Between  $250$  and  $700^\circ\text{C}$  there was an extreme loss of mass for IIPs to  $77.86\%$  and Hg-IIPs to  $83.4\%$ , from loss of several functional groups containing oxygen and of major organic compounds converted to  $\text{CO}_2$  and steam. Furthermore, at temperatures exceeding  $700^\circ\text{C}$  the masses were relatively stable up to  $998^\circ\text{C}$ . The remaining mass for IIPs was  $21.18\%$ , and for Hg-IIPs it was  $15.67\%$  of the initial mass. These results indicate that the presence of Hg(II) in the polymers can improve thermal stability compared to the absence of Hg(II).

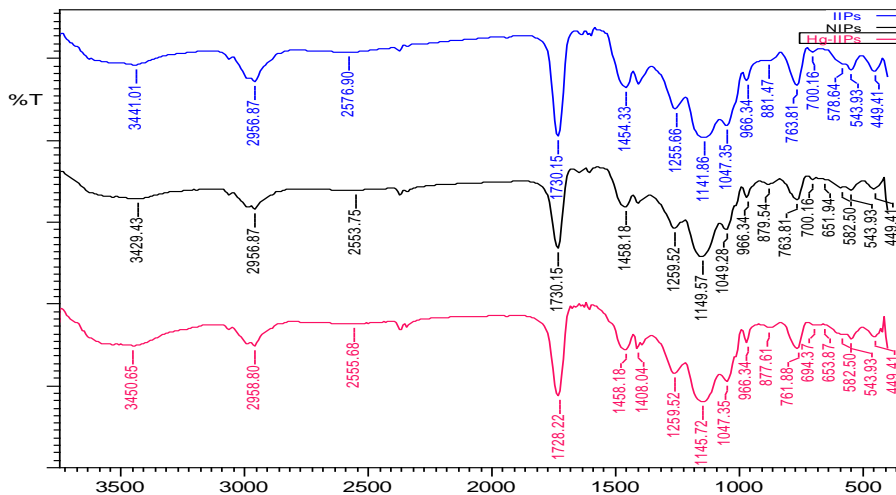


Figure 2. The FTIR spectra: Hg-IIPs (red curve), NIPs (black curve), and IIPs (blue curve).

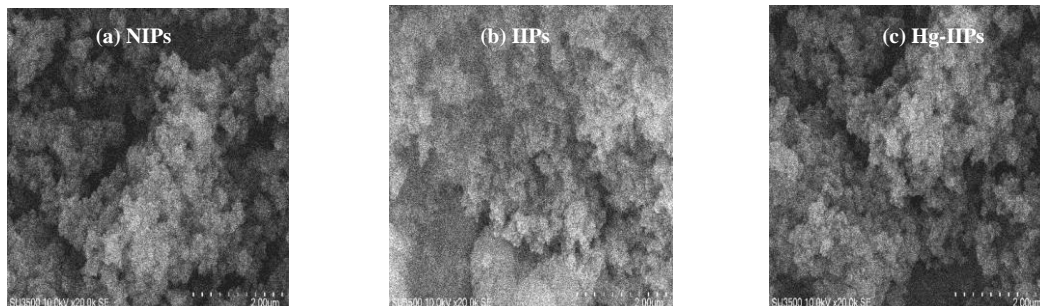


Figure 3. SEM images (20,000X magnification): (a) NIPs, (b) IIPs, and (c) Hg-IIPs.

Table 1. EDS measurement results: NIPs, IIPs, and Hg-IIPs.

Elements	Energy (keV)	NIPs		IIPs		Hg-IIPs		
		% mass	% atom	% mass	% atom	% mass	% atom	
C	K	0.277	67.57	76.6	52.4	71.87	60.76	71.15
O	K	0.525	21.19	18.04	18.37	18.91	24.61	21.63
Si	K	1.739	9.74	4.72	9.81	5.75	12.92	6.47
S	K	2.307	1.5	0.64	4.34	2.23	1.7	0.75
Hg	M	2.195	0	0	15.08	1.24	0	0

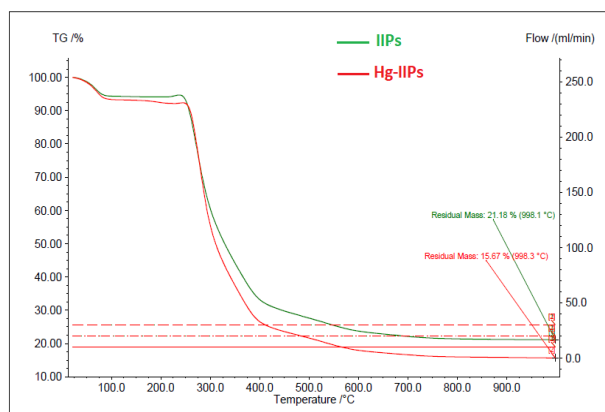


Figure 4. The TGA curves for IIPs (green curve) and Hg-IIPs (red curve).

### 3.1.4 Brunauer-Emmett-Teller (BET) analysis

BET analysis was used to determine the surface area, the total pore volume, and the average pore radius of Hg-IIPs, NIPs, and IIPs, based on the adsorption of nitrogen gas. The results from BET analysis are summarized in Table 2, where Hg-IIPs have larger surface area, total pore volume, and average pore radius than NIPs and IIPs. These results were confirmed from SEM images, clearly leaching off Hg(II) caused porosity of Hg-IIPs and increased specific surface over those of NIPs and IIPs. These are decisive factors affecting the adsorption performance of a sorbent.

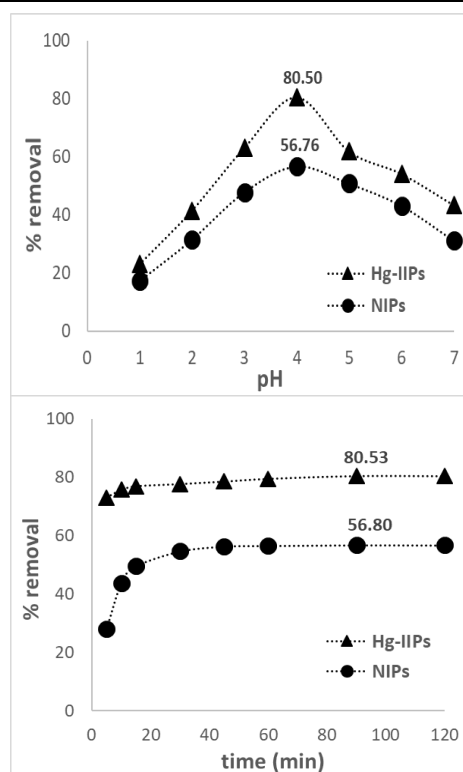
## 3.2 Characterization of removing mercury ions from aqueous solutions

### 3.2.1 Effect of pH

The effect of pH on 50 mg Hg-IIPs and NIPs with Hg(II) 40 mg.L<sup>-1</sup> during a 120 min interaction time is shown in Figure 5. At pH < 4, the ability of Hg-IIPs and NIPs to remove mercury ions was degraded, because the active groups in sorbents such as SH, Si-O-Si, and Si-OH have undergone protonation due to the high concentration of H<sup>+</sup> ions in solution. This makes the sorbent surfaces positively charged, causing electrostatic repulsion of the positively charged metal ions. Although there has been a reduction in removal at pH > 4, the metal ions begin to form hydroxylated complexes against metal hydroxide formation (Irani, Keshtkar, & Mousavian, 2011; Wu *et al.*, 2010). At pH 4 the optimum removal for Hg-IIPs was by 80.5% (16.1 mg.g<sup>-1</sup>) and NIPs were removed by 56.76% (11.35 mg.g<sup>-1</sup>), as the mercury ions in

Table 2. The results of the BET analysis: Hg-IIP, NIPs, and IIPs.

Sorbents	Surface area (m <sup>2</sup> .g <sup>-1</sup> )	Total pore volume (cc.g <sup>-1</sup> )	Average pore radius (nm)
Hg-IIPs	118.05	0.163	2.76
NIPs	28.04	0.028	1.99
IIPs	5.85	0.026	1.82

Figure 5. The effects of pH and interaction time on adsorption capacity ( $q_e$ ) for Hg-IIPs and NIPs.

solution were in the forms Hg<sup>2+</sup> and Hg(OH)<sup>+</sup>, which are highly favored by the negatively charged active sorbents.

### 3.2.2 Effect of interaction time

The effect of the interaction time with 50 mg of Hg-IIPs and NIPs, and Hg(II) 40 mg.L<sup>-1</sup> at pH 4 is shown in Figure 5. The results show that an appropriate interaction time for Hg-IIPs and NIPs was 90 min, and removal was by 80.53% (16.11 mg.g<sup>-1</sup>) for Hg-IIPs, and by 56.80% (11.36 mg.g<sup>-1</sup>) for NIPs. The effects of interaction time fall into three

stages, namely in the first 15 min there was high affinity of the active groups of the sorbent to Hg(II) ions, due to sufficient capacity, but after 15 min the sorption slowed down. At times beyond 90 min there was no more adsorption, showing that the active groups of the sorbent has been saturated by Hg(II) ions (Irani *et al.*, 2011).

### 3.2.3 Determination of optimum adsorption capacity

Figure 6 shows the optimum adsorption capacities, in terms of adsorption capacity ( $q_e$ ) curves versus the initial concentration ( $C_0$ ) of Hg(II). The optimum adsorption capacities of Hg-IIPs and NIPs were obtained with an initial concentration of  $350 \text{ mg.L}^{-1}$ , at  $62.27 \text{ mg.g}^{-1}$  for Hg-IIPs and  $28.91 \text{ mg.g}^{-1}$  for NIPs, respectively. The imprinted ions in Hg-IIPs were able to increase the optimum adsorption capacity, when the removal of mercury ions is compared to NIPs without the ionic imprints. The mechanisms of the memory effects involve size, geometry, amount of coordination, and charge of metal ions, leading to high interactions with metal ions having ligands, and resulting in increased adsorption capacity (Singh *et al.*, 2009). The advantages of Hg-IIPs in this study are founded on use of silica as core of the polymer to provide superior rigidity with excellent mechanical and chemical resistances, and the surface is easily functionalized with organosilane compounds such as MPTS (Mercier & Pinnavaia, 2000). The use of MPTS as a ligand is advantageous to the adsorption of many heavy metals (Irani *et al.*, 2011; Wu *et al.*, 2010). For comparison, Table S-2 summarizes the maximum adsorption capacities in this current study that are significantly better than with Hg-IIPs synthesized and applied to mercury ions in prior studies.

### 3.2.4 Effect of sorbent dose

Figure 7 shows the effect of sorbent doses of Hg-IIPs and NIPs on removal of Hg(II)  $40 \text{ mg.L}^{-1}$  at pH 4 for 90 min. The two sorbents gave the highest adsorption capacity ( $q_e$ ) at 25 mg sorbent dose, with  $26.03 \text{ mg.g}^{-1}$  for Hg-IIPs and  $17.22 \text{ mg.g}^{-1}$  for NIPs. On using higher sorbent doses of up to 100 mg, the adsorption capacity was smaller but the removal increased to 95.21% for Hg-IIPs and to 73.56% for NIPs. Based on this, it can be concluded that the effect of the sorbent doses of Hg-IIPs and NIPs on the removal of Hg(II) ions is that a higher sorbent dose gives a higher removal of Hg(II) ions in the environment. However, the effectiveness is then not good because the adsorption capacity gradually decreases with dose and the sorbent use is inefficient (Phet phaisit, Wapanyakul, Chaiyasith, & Sriprang, 2018).

### 3.2.5 Selectivity

The selectivity of Hg-IIPs to Hg(II) for Hg in the presence of Pb(II), Cd(II), and Cu(II) is shown in Figure 8, where the results show that Hg-IIPs was selective for Hg(II) in the presence of Pb(II), Cd(II), and Cu(II) in all three types of solutions, namely single ion type, binary, or quaternary; and the rank order of separation levels was  $\text{Hg/Cu} > \text{Hg/Cd} > \text{Hg/Pb}$ . In the quaternary solutions, separation was stronger than with single and binary solutions, and the selectivity coefficient was 46.92 for Hg/Cu, 16.82 for Hg/Cd, and 2.07 for Hg/Pb. These results indicate the effectiveness of the

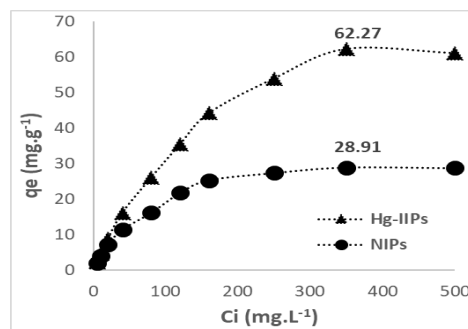


Figure 6. The initial concentration ( $C_i$ ) versus adsorption capacity ( $q_e$ ) for determining the optimum adsorption capacities on Hg-IIPs and NIPs.

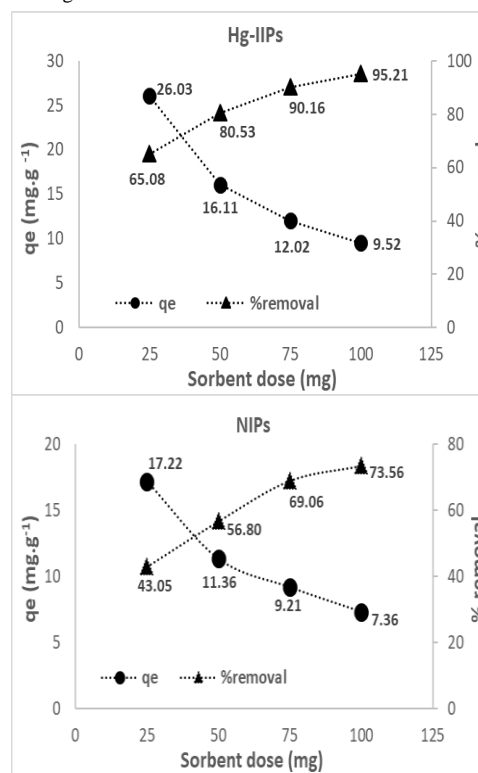


Figure 7. Effect of the sorbent dose of Hg-IIPs or NIPs on adsorption capacity and percentage removed.

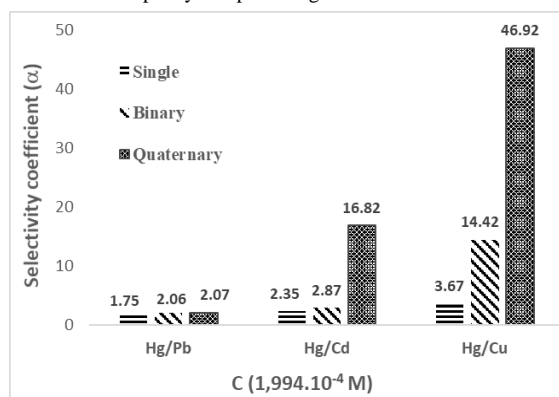


Figure 8. Selectivity coefficient ( $\alpha$ ) of Hg-IIPs for Hg(II) ions in the presence of Pb(II), Cd(II), and Cu(II) ions.

cavities generated by imprinting Hg(II) in Hg-IIPs, where the ion size greatly influences adsorption of a metal ion. The smaller the ion size was, competing with Hg(II), the larger was the coefficient of selectivity, even though Pb (II), Cd (II), and Cu(II) have similar electric charges as Hg(II) (Hashemi *et al.*, 2015).

#### 4. Conclusions

The Hg(II)-ion imprinted polymers (Hg-IIPs) with silica core were synthesized for use as sorbents to remove mercury ions, by radical polymerization using complexes of Hg(II) ions with MPTS ligands as a template, VTMS as monomer, and EGDMA as crosslinker in the molar ratio 1: 6: 6. The Hg-IIPs as sorbent removed mercury ions optimally from a batch at pH 4 with an interaction time of 90 min and with optimum adsorption capacity of 62.27 mg.g<sup>-1</sup>. The imprints of ions in Hg-IIPs improved the optimum adsorption capacity of the sorbent for the removal of mercury ions, from that of NIPs without ionic prints. The selectivity of Hg-IIPs for Hg(II) in the presence of Pb(II), Cd(II) and Cu(II) was highest with a quaternary solution, and the selectivity coefficients were 46.92 for Hg/Cu, 16.82 for Hg/Cd, and 2.07 for Hg/Pb. This study indicates that Hg-IIPs could be very important for mercury analysis in industrial applications, including separation, environmental remediation, preconcentration, or the development of instruments.

#### References

- Bershtein, V., Gun'ko, V., Egorova, L., Guzenko, N., Pakhlov, E., Ryzhov, V., & Zarko, V. (2009). Well-defined silica core-poly(vinyl pyrrolidone) shell nanoparticles: Interactions and multi-modal glass transition dynamics at interfaces. *Polymer*, 50, 860-871.
- Coates, J. (2006). Interpretation of infrared spectra, a practical approach. *Encyclopedia of Analytical Chemistry* (pp. 13-15). Hoboken, NJ: John Wiley and Sons.
- Didi, M. A., Medjahed, B., & Benaoudam, W. (2013). Adsorption by liquid-liquid extraction of Hg(II) from aqueous solutions using the 2-butyl-imidazolium di-(2-ethylhexyl) phosphate as ionic liquid. *American Journal of Analytical Chemistry*, 4, 40-47.
- Escudero, L. B., Olsina, R. A., & Wuilloud, R. G. (2013). Polymer-supported ionic liquid solid phase extraction for trace inorganic and organic mercury determination in water samples by flow injection-cold vapor atomic absorption spectrometry. *Talanta*, 116, 133-140.
- Firouzzare, M., & Wang, Q. (2012). Synthesis and characterization of a high selective mercury(II)-imprinted polymer using novel aminothiols monomer. *Talanta*, 101, 261-266.
- Ghazy, S. E., El-Reash, G. M. A., Al-Gammal, O. A., & Yousef, T. (2010). Flotation separation of mercury(II) from environmental water samples using thiosemicarbazide derivatives as chelating agents and oleic acid as surfactant. *Chemical Speciation and Bioavailability*, 22, 127-134.
- Hashemi, B., Shamsipur, M., Javadi, A., Rofouei, M. K., Shokravi, A., Tajarrud, N., & Mandumy, N. (2015). Synthesis and characterization of ion imprinted polymeric nanoparticles for selective extraction and determination of mercury ions. *Royal Society of Chemistry (Analytical Methods)*. doi:10.1039/c5ay02545a.
- Irani, M., Keshtkar, A. R., & Mousavian, M. A. (2011). Removal of Cd(II) and Ni(II) from aqueous solution by PVA/TEOS/TMPTMS hybrid membrane. *Chemical Engineering Journal*, 175, 251-259.
- Mercier, L., & Pinnavai, T. J. (2000). Direct synthesis of hybrid organic-inorganic nanoporous silica by a neutral amine assembly route: structure-function control by stoichiometric incorporation of organosiloxane molecules. *Chemistry of Materials*, 12(1), 188-196.
- Phetphaisit, C. W., Wapanyakul, W., Chaiyasith, W. C., & Sriprang, N. (2018). Selective adsorption of indium ions on polyacrylamido-2-methylpropane sulfonic acid-grafted-natural rubber. *Songklanakarin Journal of Science and Technology*, 40(5), 1167-1174.
- Piletsky, S. A., Turner, N. W., & Laitenberger, P. (2006). Molecularly imprinted polymers in clinical diagnostics-future potential existing problem. *Medical Engineering and Physics*, 28, 971-977.
- Risher, J. F., & Amler, S. N. (2005). Mercury exposure: Evaluation and intervention the inappropriate use of chelating agents in the diagnosis and treatment of putative mercury poisoning. *Neurotoxicology*, 26, 691-699.
- Roushani, M., Abbasi, S., & Khani, H. (2015). Synthesis and application of ion-imprinted polymer nanoparticles for the extraction and preconcentration of mercury in water and food samples employing cold vapor atomic absorption spectrometry. *Environmental Monitoring and Assessment*, 187, 601. doi:10.1007/s10661-015-4820-z.
- Singh, D. K., & Misrah, S. (2009). Synthesis of new Cu(II)-ion imprinted polymers for solid phase extraction and preconcentration of Cu(II). *Chromatographia*, 70, 1539-1545.
- Soleimani, M., Mahmodi, M. S., Morsali, A., Khani, A., & Afshar, M. G. (2011). Using a new ligand for solid phase extraction of mercury. *Journal of Hazardous Materials*, 189, 371-376.
- Urgun-Demirtas, M., Benda, P. L., Gillenwater, P. S., Negria, M. C., Xiong, H., & Snyder, S. W. (2012). Achieving very low mercury levels in refinery wastewater by membrane filtration. *Materials*, 215, 98-107.
- Wu, S., Li, F., Wang, H., Fu, L., Zhang, B., & Li, G. (2010). Effects of poly (vinyl alcohol) (PVA) content on preparation of novel thiol-functionalized mesoporous PVA/SiO<sub>2</sub> composite nanofiber membranes and their application for adsorption of heavy metal ions from aqueous solution. *Polymer*, 51, 6203-6211.
- Wulandari, M., Urraca, J. L., Descalzo, A. B., Amran, M. B., & Moreno-Bondi, M. C. (2015). Molecularly imprinted polymers for cleanup and selective extraction of curcuminoids in medicinal herbal extracts. *Analytical and Bioanalytical Chemistry*, 407, 803-812.